Stephen Kenyon
Physics 460
Dr. Andresen
4/29/15

Construction of Magnetic Tweezers for use in Single Molecule Experiments

Abstract: Magnetic Tweezers represent a powerful and experimentally simple tool for force spectroscopy of DNA and other single molecules, and allow for piconewton forces and nanometer position resolution. A set of magnetic tweezers were constructed at Gettysburg College. Their design, use, and limitations are presented, along with recommendations for improving the experimental viability of the tweezers design at Gettysburg.

I. Introduction

Force plays a fundamental role in many biological processes, such as in the replication and transcription of DNA.[1] DNA is highly wound and compact in our bodies, and force plays a role in both the packing and unpacking of DNA in our cells.[1] Force spectroscopy techniques such as magnetic tweezers (MT) provide a powerful and experimentally simple method for resolving the force involved in extending nucleic acids such as DNA or RNA.[1,2,3] In addition to resolving the force involved in the extension of these nucleic acids, MT can also be used to resolve forces involved in extending these nucleic acids under different conditions, such as when they are acted on by an enzyme, or under different salt conditions.[1,4,5] Also, MT can also be used to apply torque to a nucleic acid and resolve the effects of torque on the molecule on its extension.[6]

A magnetic tweezers apparatus consists of an inverted microscope with a pair of magnets (either permanent or electromagnetic) placed above a flow cell that can be used to manipulate paramagnetic beads attached to the molecule to be studied.[1] Light is shone through the magnets illuminating the sample placed in the flow cell below. An image is magnified in an objective and then redirected and focused onto a CCD for image collection and analysis. From these images of

the bead being acted upon by the magnetic force, we can determine the behavior of the molecule of interest under force-extension experiments.[7,8]

In this paper I present the theory of magnetic tweezers operation for use in single molecule experiments. I also detail the construction of MT built at Gettysburg College during the summer of 2014. Finally, I present an overview of MT operation for the tweezers at Gettysburg College.

II. Theory Overview

MT have two primary variations. In one, electromagnets are employed as force clamps, whereas in the other a pair of permanent magnets are used as the force clamps.[1,9] The tweezers implemented at Gettysburg utilize a pair of permanent neodymium magnets with a field strength as high as 1.48 Tesla. The opposite poles on each of the magnets face each other and are separated by a gap ~1mm. The magnetic field strength decays roughly exponentially (see calculation of force) according to the separation of the magnets.[10] Permanent magnetic tweezers are apt for performing constant force experiments, but are unable to manipulate beads in three dimensions.[9]

The molecule to be studied (typically double stranded DNA) is tethered on one end to a flow cell, with a streptavidin coated paramagnetic bead attached to the other end.[1] The flow cell is mounted on an inverted microscope, with the magnets placed above the flow cell to apply force on the beads.[1]

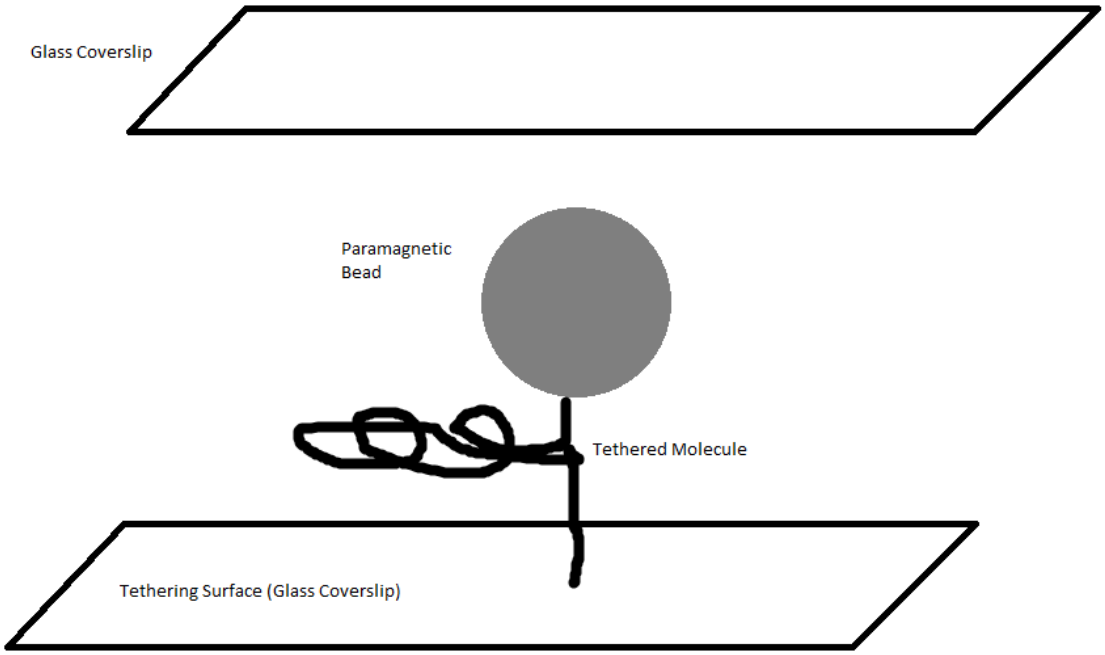

Figure 1: Inside the Flow Cell, not to scale. The molecule of interest is tethered to one end of the flow cell, a glass coverslip. The other end is tethered to a paramagnetic bead. Another coverslip completes the chamber. The bead is several orders of magnitude larger than the molecule, approximately 1 – 2 microns in size, while the molecule is typically thousands of base pairs long. When imaging the flow cell, only the bead is seen.

The position of the bead can be measured in real time through imaging with a CCD camera via video microscopy.[7,8] The main advantage of the use of video microscopy is the lack of additional equipment needed besides the camera and image system hardware.[8] All of the position tracking can be done in real time through the use of software. For the program used in this version of MT, it is possible to find X, Y, and Z positions within an accuracy of 10nm.[10]

There are a variety of bead tracking methods, with algorithms designed to track both single beads and multiple bead ensembles.[7] Such methods include algorithms that perform a direct calculation of the sub-pixel location, and algorithms that compare an image to a control image (either a previous image or some predefined image). Two example methods for each are algorithms that primarily look for a center of mass or centroid (COM) for direct calculation of the sub-pixel location, and cross-correlation method (XCORR) for previous image analysis.[8]

The COM algorithm is computationally non-intensive, but is not used in our implementation of the tweezers. However, as a reference, the position for X, or Y is given as

$$X_{COM} = \frac{\sum_{i=1}^{n}\sum_{j=1}^{n}(iI_{ij*})}{\sum_{i=1}^{n}\sum_{j=1}^{n}I_{ij*}} \quad (1)$$

where i and j are an integer x and y coordinate in an n by n image. I_{ij*} is the absolute value of the subtracted median intensity: $I_{ij*} = \left|I_{ij} - I_{med}\right|$. For the XCORR, the method is based by selecting a band of pixel rows from the image and cross correlating the average intensity profile with its own mirror profile (ie from an original or previous image of these pixels). As an example from van Loenhout (8), a band is averaged around 0.2pixels about the image center line:

$$P(i) = \frac{1}{0.2n}\sum_{j=0.4n}^{0.6n} I_{ij}, \quad (2)$$

and then is cross correlated with its mirror image in Fourier space:

$$C_{xx} = IFFT(FFT\big(P(i)\big) * \{FFT(P(-i))\}^{*}.^{8} \quad (3)$$

In simpler terms, the intensity profile of the region of choice is compared to all other regions in the image throughout time. A match in the cross correlation between the two images would denote where the bead exists in translational space.

For the Z position of the bead, a lookup table (LUT) of radial profiles is generated by moving the objective in a sequence of known steps. A stack of images is generated by changing the focus of the objective in about 200 steps at 100nm per step. The LUT is created by calculating the radial profile at each position of the objective. COM or XCORR can be used to

map the pixel intensities. To determine the Z position of the bead in any given image, the χ^2 difference of the radial profile with the planes of the LUT are created. The minimum χ^2 difference gives the best matching radial profile and from that the best corresponding Z position.[8]

An issue arises when trying to determine the Z position of the bead when the index of refraction of the flow cell differs from the index of refraction with the objective, as a movement in the objective does not correspond 1:1 with a movement of a bead. This is true in our case, as we are using an oil immersion objective ($n_{oil} = 1.51$, $n_{water} = 1.33$). The small angle approximation for a correctional conversion factor is not appropriate however, for objectives with high numerical aperture, and needs to be determined experimentally.[8]

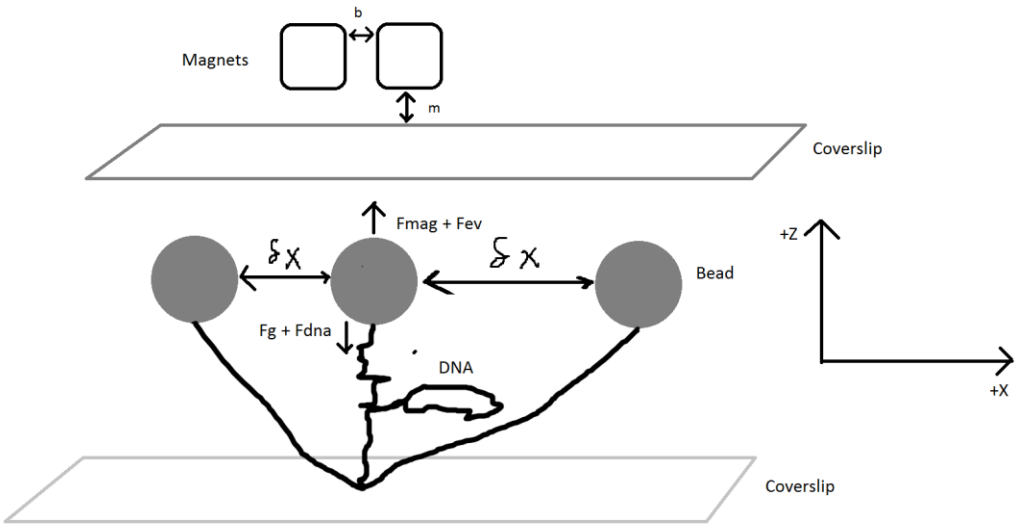

Figure 2: Flow Cell Action Diagram, not to scale. The forces acting on the bead are Fmag, Fev, Fg, and Fdna, where Fmag is the magnetic force acting upward, and Fev are any volume effects not considered. Fg is the gravitational force (assumed small) and Fdna is the tension of the DNA. Displacements in the x position (parallel to the coverslip) are shown. The distance of the magnets to the flow cell is given as m, and b is the magnet separation.

In a constant force measurement, the force of the magnet is given by:

$$F = k_B T \frac{\langle z(t) \rangle}{\langle (\bar{x} - x(t))^2 \rangle} \tag{4}$$

where $k_B T$ is the thermal energy, $\langle z(t) \rangle$ is the average vertical position of the bead, and the denominator is the fluctuations of the bead in the transverse (x) direction.[10] A plot of this force against the displacement of the bead should follow the worm-like chain model for DNA:

$$F_{DNA}(z) = \frac{k_B T}{p} \left\{ \frac{1}{4(1 - \frac{z}{L_O})^2} - \frac{1}{4} + \frac{z}{L_O} \right\} \tag{5}$$

where p is the fitted persistence length (on the order of 48 nm), L_O is the fitted contour length (on the order of microns), and z is the extension.[11] For a dynamic force measurement where the magnets trace a trajectory, the total force decays exponentially as a function of the magnet position:

$$F_{total} = F_{mag} e^{-m/b} + F_O \tag{6}$$

Where F_{mag} is the maximum force, m is the magnet position relative to the flow cell, b is the separation of the magnets, and F_O is a constant offset to account for excluded volume effects and gravity. F_O is typically on the order of 27 to 31 fN.[10, 12]

Magnetic tweezers can also be used to measure the torque and torsional stiffness for a molecule such as DNA. The setup in the flow cell is the same as when measuring force. By

rotating the magnets, a torque can be applied to the bead, and likewise the tethered molecule. The torsional stiffness k_{rot} of the trapped molecule is given by

$$k_{rot} = \frac{k_b T}{\langle \delta\theta^2 \rangle}, \tag{7}$$

where $\langle \delta\theta^2 \rangle$ are the rotational thermal fluctuations of the bead.[6] If the molecule is either overwound or underwound it will exert a restoring torque on the bead:

$$\tau_{DNA} = -k_{rot}\langle \theta - \theta_O \rangle. \tag{8}$$

Here, θ_O is the equilibrium angle of the bead.[6] Again, there is the issue with actually measuring the displacement angle, which is once again achieved by video microscopy. Several methods exist for the viewing of the rotation angle of the bead. One such method involves the attachment of a non-magnetic, biotinylated bead to a streptavidin coated paramagnetic bead.[9] In this instance, the non-magnetic bead is smaller than the paramagnetic, and the paramagnetic once again takes on the role as the upper tether for the molecule being studied. The smaller bead allows for the direct tracking of the rotation angle while simultaneously tracking the paramagnetic bead's x, y, and z coordinates.

III. Gettysburg Tweezers Design

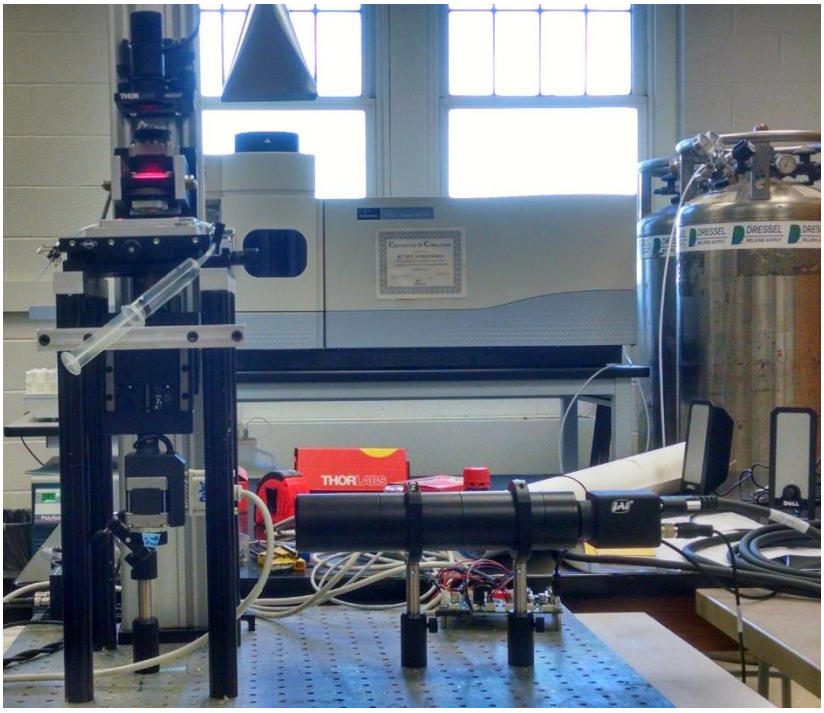

Figure 3: Gettysburg Magnetic Tweezers.

The tweezers design implemented at the college is similar to the one as described in Kruitof et. al (10). This section will describe the current standing of the tweezers at Gettysburg College starting with the light source and ending at the point of computer input (Top-Down).

The light source consists of a red, 625nm LED supplied by Thorlabs. The wavelength of the light was chosen primarily due to cost constraints. The light coming off the LED is collimated using an aspheric condenser (f = 20mm). An LED current driver (Thorlabs, LEDD1B T-Cube, max current 1200mA) is used to moderate the intensity of the light emitted by the LED. In general, collimated light is used in order to produce good, well-defined concentric diffraction rings around the beads for use in determining the bead position, both lateral and axial.

For good viewing of images of the flow by the computer via the CCD, the driver is set to about two-thirds max power. More intense light will white-out the image appearing on the computer screen of the sample cell; likewise too dark of a light source will also make it difficult to see a proper image of the sample cell. It is important that the light source be bright enough to illuminate the sample cell in order to see both the beads in the cell and the diffraction rings of the beads produced by the collimated light.

Figure 4: LED and Rotary Motor Apparatus. The LED is attached to rails in the background. An attachment piece for the LED was machined with a slot to allow for horizontal positioning. Additional alignment is achieved through the kinematic mount and rail positioning.

Directly beneath the LED setup is the magnet holder/rotary motor setup. A machined magnet holder is attached to a rotary stepper motor (Owis Rotary Stages, DRTM 40). This rotary motor is in turn attached to a custom built piece to couple the rotary motor to a stepper motor (PI M-126 Series Linear Positioning Stages) (referred to as stepper rot and stepper shift in the LabVIEW code, respectively) that moves in the vertical direction.

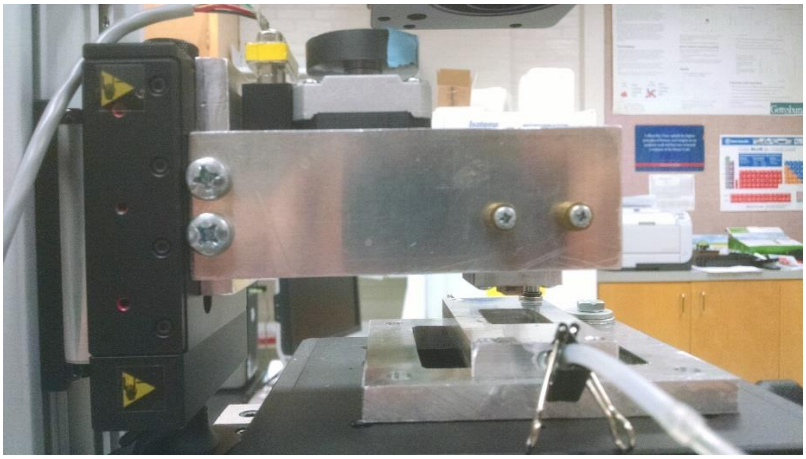

Figure 5: Stepper Rot and Stepper Shift. The vertical positioning motor for the magnets (stepper shift) is positioned on the rails so that near the lowest height of the magnets on the stepper shift's descent corresponds to the magnets coming into contact with the flow cell. In its current configuration, the flow cell is too thick to allow for contact, and needs to shaved down.

The magnets are spaced about 1mm apart, with pole-opposite orientation. A 1mm through hole is placed in the holder at the same location as the space between the magnets so as to allow the LED light to shine through. The magnets are held to the holder using epoxy.

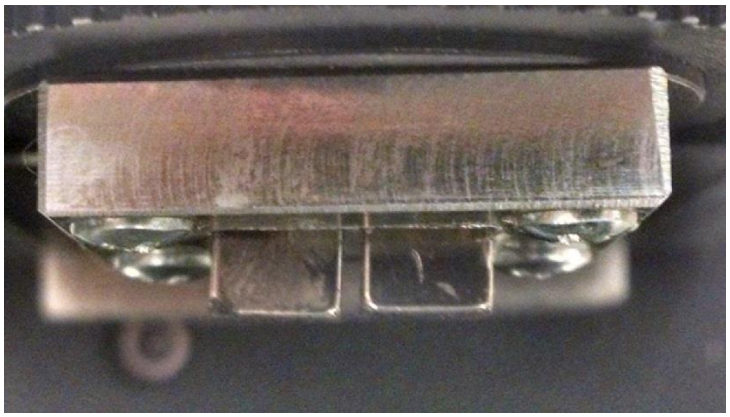

Figure 6: Magnet Holder and Magnets. The Nd magnets exert an exceptionally strong magnetic field. When setting the magnets into the holder, precautions need to be made to ensure that the magnets do not collapse in on themselves. Initially, the magnets were held with a glue weaker than the current epoxy, and collapsed after about one month. Spacing was achieved with pieces of paper in between the magnets while the epoxy dried.

The previous elements of the tweezers listed are all attached to 95mm rails (Thorlabs) to allow for customization of the placement in vertical space. When aligning the mounting of the magnet/rotary and stepper shift motor apparatus, only one consideration needs to be taken into

account; mainly, does the range of stepper shift in its current configuration allow for the magnets to come into physical contact with the flow cell (for calculation of the maximum magnetic force on the beads, as described previously). The mounting constraint for the LED is primarily an issue of optical alignment; the top of the objective needs to be illuminated by the LED in all cases, even when the magnets are rotating.

Below the magnets/stepper rot and shift configuration is an XY table with a custom built flow cell attached above it. The flow cell consists of a rectangular piece of aluminum with a channel cut in the center. Two glass cover slips cover the end of either side of the flow cell, with PDMS (polydimethylsiloxane) filling the space in between the glass cover slips, save for the channel. Two drill holes on either end of the cell allow for tubes to be placed in them, allowing for fluid to be flown into and out of the cell. The XY table is attached to a custom built mount, approximately 14 inches above the breadboard and is independent of the rails which hold the magnets/ rotary and shift motors, and the light source.

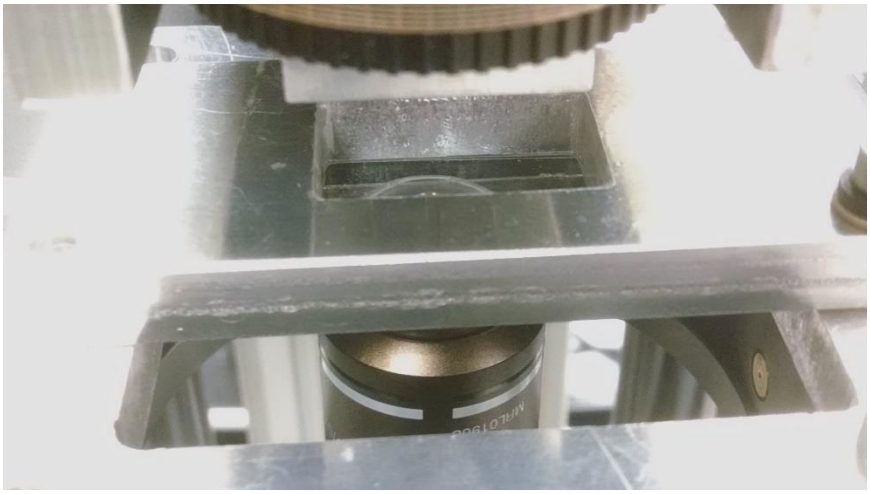

Figure 7: Objective and Flow Cell. After preparing the flow cell it is placed removable-cover slip side down on the holder on the XY table. The objective is able to touch the flow cell without damaging the cell or the objective itself. Since the objective is oil immersion, it is able to come into physical contact with the flow cell. Since the optics are set in, there exists a little bit of metal above the optics. The flow cell should however not be raised too high into the flow cell, as this risks shattering.

Beneath the flow cell is a 100x oil immersion Nikon microscope objective. The objective is coupled to another vertically moving stepper motor, listed as stepper focus in the LabVIEW code. The stepper focus motor is coupled to the custom built mount, as described above.

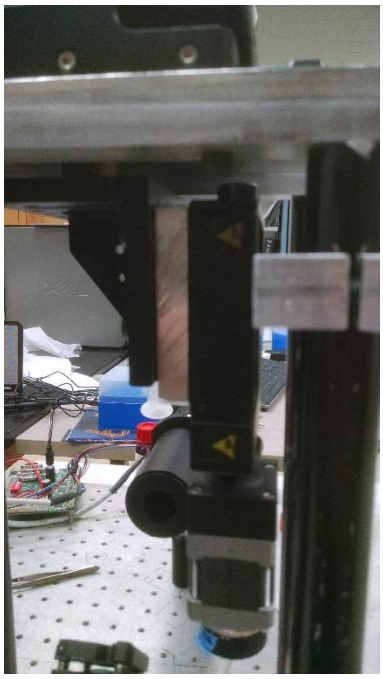

Figure 8: Stepper Focus and Objective Holder.

All of the motors described are connected to the motor controller board (Trinamic TMCM-6110), which is in turn connected to the computer via USB.

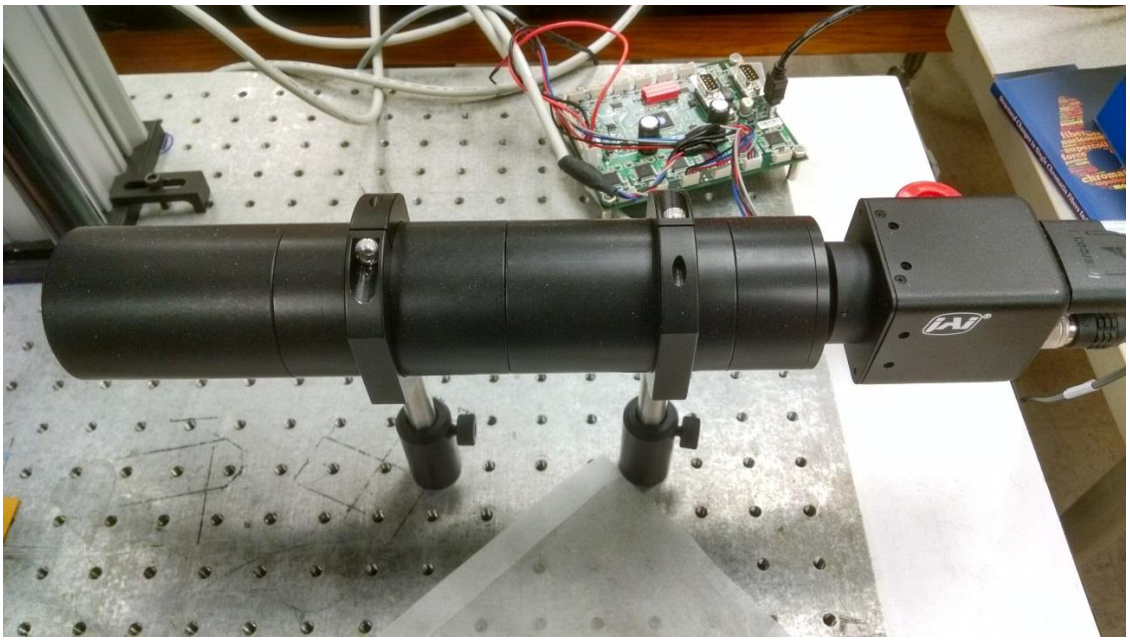

Figure 9: Lens Tube, Camera, and Control Board. The lens tube is for 2 inch diameter lenses. The CCD is coupled to the end of the tube using a 2 to 1 inch converter. In the background is the TMCM 6110.

Light exiting the back end of the objective is redirected by a 45° mirror into a lens tube. Light coming into the tube is focused by a lens (f = 100mm) onto a CCD (Jai-Pulnix RM-6740CL). The CCD is linked to the computer via a frame grabber.

a. Computer Control of Tweezers and Documentation of TweezersJ11_S

The Gettysburg tweezers operate from a modified version of LabVIEW code supplied by John van Noort of Leiden University. Most of the work done on the code supplied by John van Noort was to update it, or essentially "port it" to our version of the tweezers. There were three main differences that needed to be rectified or accounted for when porting the code to our version of MT. First, the original version of the code supported syringe pumps, and piezo electric motors, which we currently are not using. These portions of the code needed to be disabled. Second, our tweezers use stepper motors in places where van Noort's used piezos, which meant that we had to update the motor control portion of the code to reflect this difference. Last, there

were minor differences in the frame rate for our CCD and the original CCD that the code needs to account for.

The largest part of the changes occurred in SimpleMove.vi, which controlled all of the motor movements. In the unaltered version of the code, Stepper Rot and Stepper Shift were originally controlled as a separate case structure, since they were originally piezo-electric devices. The control of the movement of these motors was changed to be handled by the same portion of code that control the other stepper motors. Thus, all motors move from the same case structure within SimpleMove.vi. This however allows for the future possibility of acquiring piezo electric devices to be used in place of stepper motors for Stepper Shift and Stepper Focus, as the code controlling these devices has merely been diagram-disabled.

The LabVIEW code serves two main functions. First, the code provides a method for accurately controlling the movement of the objective, allowing for a quick and easy method of changing the object in the flow cell focused on. This motor control is also extended to control for the placement of the magnets in vertical space and their rotation, allowing for automation of both of these processes. Second, the code allows for control of the data received from the CCD, and for its interpretation through the use of a look-up table (LUT).

The code is capable of passing two types of moves to the motors: relative move and absolute move. In relative move, the motor receiving the move order moves the distance passed to it via command, regardless of where it exists currently. In absolute move, the motor is given a position to move to, regardless of how far away it might be from that position. In either case, there exists a need to know how to convert from “board units”, which in this case would be the number of steps a stepper motor would take to complete a move, into physical distance.

Values of the gain for stepper rot, stepper shift, and stepper focus can be found and modified in the Calib.txt file. Also in this file it is possible to alter values for the allowed range of the motors, so as to avoid crashing into the flow cell, or passing a command to the motor to move outside of its possible range, which will damage the motor.

It is possible to change other motor values, such as the max current, standby current, max speed, and acceleration. The max speed of the motor is limited by both technical limitations of the motor and by the pulse divisions of the stepper motors set by the motor control board. It is possible to find these values and change them in the TMCL IDE, which is separate from the LabVIEW code. TweezersJ11_S is the main instance of the LabVIEW code that operates the tweezers. In order to properly run the program, both the motor control board and the CCD must have power.

After reworking the code to support our stepper motors and ensuring that their moves corresponded to actual physical units, much time was spent on ensuring that the code made a proper lookup table from images from the camera. The CCD supports 200Hz, while the code is hard-wired to either 40Hz or 60Hz. A work-around was achieved by using NI-MAX, a National Instruments device control program. For the CCD, the shutter pulse width control setting was changed to 6400. The manual shutter setting was changed to a value of "1". This gave a frame rate of about 86Hz, closer to the code's value of 60Hz. This workaround was later reverted, as there is believed to be an issue with the code's internal timing. This frame rate issue and the timing issue have yet to be fully revised.

b. Known Issues

Power loss to the computer, either from a restart operation or actual loss of power will result in a reset of the calibrated position of the motors with regards to physical units. Disconnecting the motor control board from its USB connection to the computer will also result in a similar effect. The reason behind this is that the motor control board is unable to save memory following a loss of power, and the absolute position of the motors in board units are reset to zero. This has the effect of creating a systematic offset when running the program again, as the previous calibration of board units to physical units is dependent upon the motors' position with regards to the control board's idea of the motors' position. An example follows which will better illustrate the problem and describe a workaround. It is possible to operate the motors through a computer interface separate from the TweezersJ11_S program. This is possible through the TMCL IDE. However, it is important to not have this program open while running TweezersJ11_S, as it may result in unresponsive motors, which could lead to crashing.

Motors that are engaged in a move order may be called to stop the move by pressing the Abort key on the front panel. This however does not always cause a motor to stop moving, so it is important at all times to consider the possible outcomes of a move before engaging in a move. If the abort key is unresponsive, it is possible to stop motors within the set of LabVIEW code by calling TMCLMotorControl.vi after exiting out of TweezersJ11_S and run the stop command for the motor that is moving. If this also fails to stop unresponsive motors, it is advisable to kill the power to the tweezers, but not the computer (do not disconnect the control board from the USB to the computer). Exit all LabVIEW programs before restarting operations.

IV. Experimental Methods

Coverslips for the tethering of beads are prepared by soaking in isopropanol for 10 minutes. Once sufficiently clean, the coverslips are blow dried in a flow of nitrogen glass. The coverslip is then placed into a glass beaker with one corner of the coverslip sticking out so that it is possible to grab it after coating. The coverslip is coated in polystyrene. A small amount of polystyrene is placed in the bottom of the beaker. A microscopy slide is used to lay along the coverslip to draw up the polystyrene. After coating, the glass is blown dry with nitrogen. The coverslip is prepared so that the coated side faces inward on the flow cell. After this, 1uL anti-digoxigen is mixed with 1mL milliQ water. The flow cell is flushed through the tubing with milliQ water. The coverslip is placed coated side down, and carefully pressed down on the PDMS with a pair of tweezers. The milliQ anti-dig mix is slowly sucked into the flow cell, about 400uL. The flow cell is then incubated for 2 hours at 4 degrees Celsius. The cell is then filled with passivation buffer (500uL 4% BSA (10X) and 500uL 2% Tween). The flow cell is then further incubated over night at 4 degrees Celsius.

During an experiment, the beads and DNA are kept in ice. 1mL of ESB(+) buffer is flown through the flow cell in order to rinse it. The cell is then placed with the coated cover slip side facing down, so that gravity causes the beads to fall to the coated coverslip. 1uL DNA in 500uL buffer is mixed, flown into the cell, and then incubated 10 minutes. 1uL Streptavidin coated beads in 500uL buffer is then flown into the cell, incubated for another 10 minutes. The flow cell is finally rinsed with 1mL buffer.

In general, it’s important to make sure that no bubbles or cracks appear when preparing the flow cell by attaching the coverslip to it. Should the glass coverslip crack and need to be changed, it can be removed by carefully pulling it away from the PDMS by using a pair of

tweezers. After removal of the coverslip, the flow cell should be flushed with isopropanol and distilled water.

The flow cell is attached to the XY table, with the prepared cover slip closest to the objective. With the TweezersJ11_S.vi running, the objective is raised to the flow cell, so that one of the stuck beads is brought slightly out of focus. A LUT is then built off of this bead.

For a dynamic force-pulling experiment, the maximum force is calibrated by placing the magnets as close as possible to the flow cell.[10] With the current design of the flow cell however, our version of the Tweezers limits the maximum force that the magnets can apply to the bead. The thickness of the aluminum portion of the flow cell prevents the magnets from actually coming into contact with the glass coverslip, so the largest maximum force cannot be achieved. Regardless, the maximum force can be found by monitoring the position of the bead with a stationary magnet position, held for one hour so as to maximize the sample size of the positions of the bead.[10] The maximum force is then found by equation (4). The dynamic force pulling experiment is then completed by creating a trajectory for the magnets to move and monitoring the position of the bead over the change in the position in the magnets. Data for this experiment were taken by a lab group in the XSIG Salty and Fatty lab. Data was analyzed post lab using the raw output data of the time, bead X, Y, and Z positions, and the magnet position as reported from the LabVIEW code.

The magnets were moved on a trajectory for a forward and backwards trace. The trace of the path of the magnets should be symmetric with time. This however, is not the case. This represents an example of a possible timing issue with the LabVIEW code, and needs to be resolved.

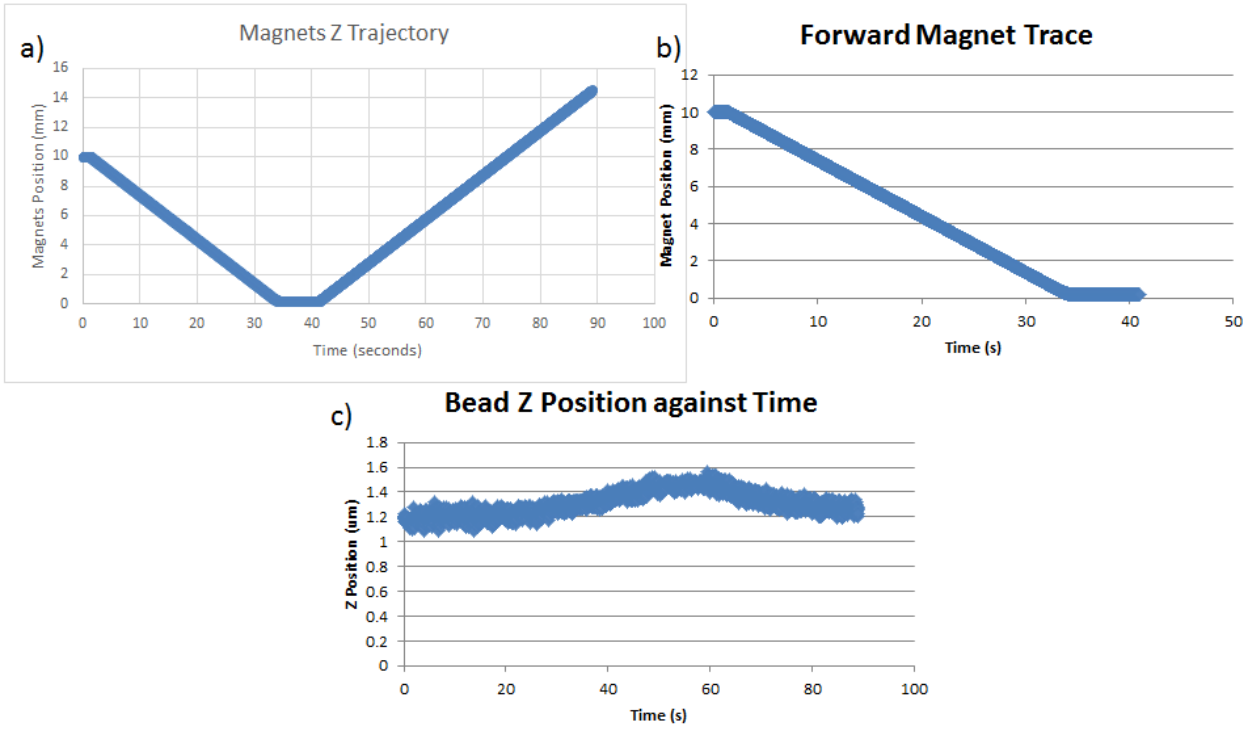

Figure 10: Magnet Trajectory and Bead Position. A) The path of the magnets as reported by the LabVIEW code. The magnets should have stopped at 10mm in the z position as this is the return position. The code did not report this as being true, however, which represents a possible timing issue. B) Shows just the forward magnet trace, and this was the only case considered in the analysis of the data. C) shows the position of the bead as the experiment was run. As the magnets moved closer to the flow cell, the beads rose in height. The highest bead position is achieved some time after the magnets are the closest to the flow cell.

V. Discussion

The maximum force was calculated from equation (4) by considering the bead fluctuations at a magnet position of 0.2mm. This was found to be F_{mag} = 1.09 pN. Using this result for F_{mag} and equation (5), it is possible to plot the force-extension curve of the DNA for the forward trace of the magnets.

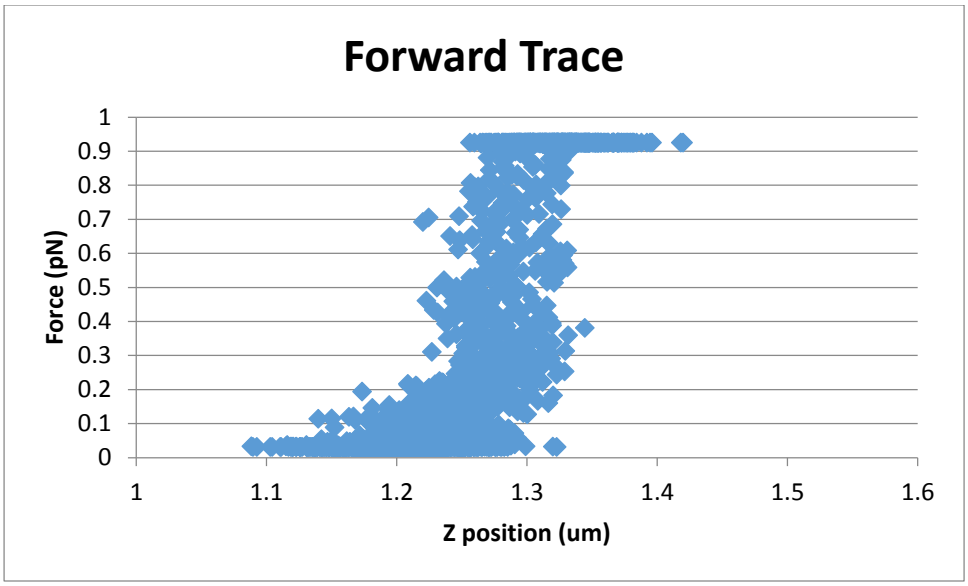

Figure 11: Force extension curve for DNA during a Dynamic Pulling Experiment. The x scale is shown from 1um to 1.6um in order to highlight the functional form of the forward trace.

We compare the force extension of the DNA found from the dynamic pulling experiment to the functional form of the worm-like chain.

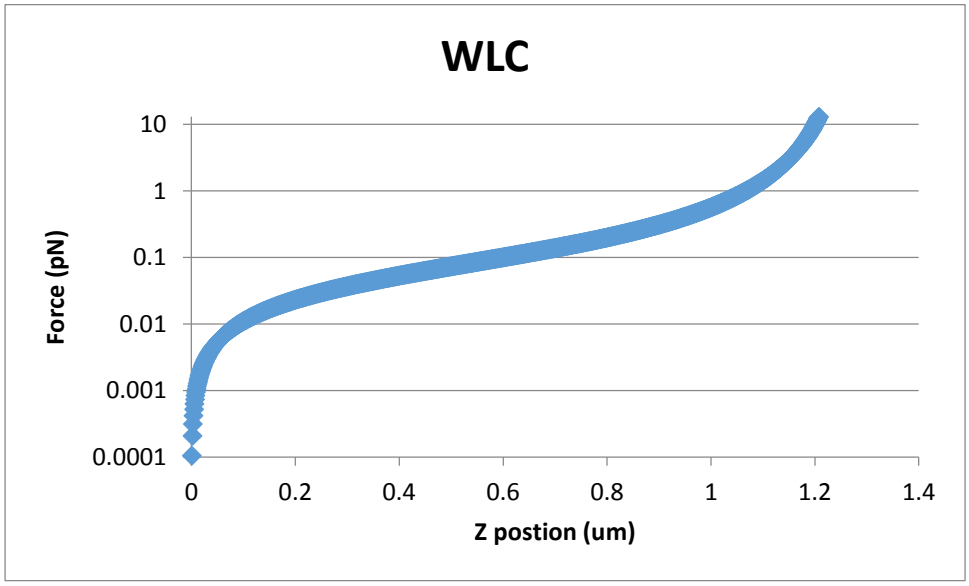

Figure 12: WLC Model for DNA Extension. We set the persistence length p = 48nm and the contour length L_o = 1.26um.

From this, two things are immediately apparent. First, the data of the forward trace is much more contracted in the Z position of the bead than what the worm-like chain would suggest. Second, it

naively appears that the results from the forward trace do somewhat match the functional form of the worm-like chain, until it is considered that Figure 12 shows the WLC on a log scale on the vertical axis. Extension of the DNA is seen, but it cannot be said that it entirely matches the form suggested by the WLC. If we consider the WLC only over the same Z position range as in Figure 11, a much clearer picture can be seen.

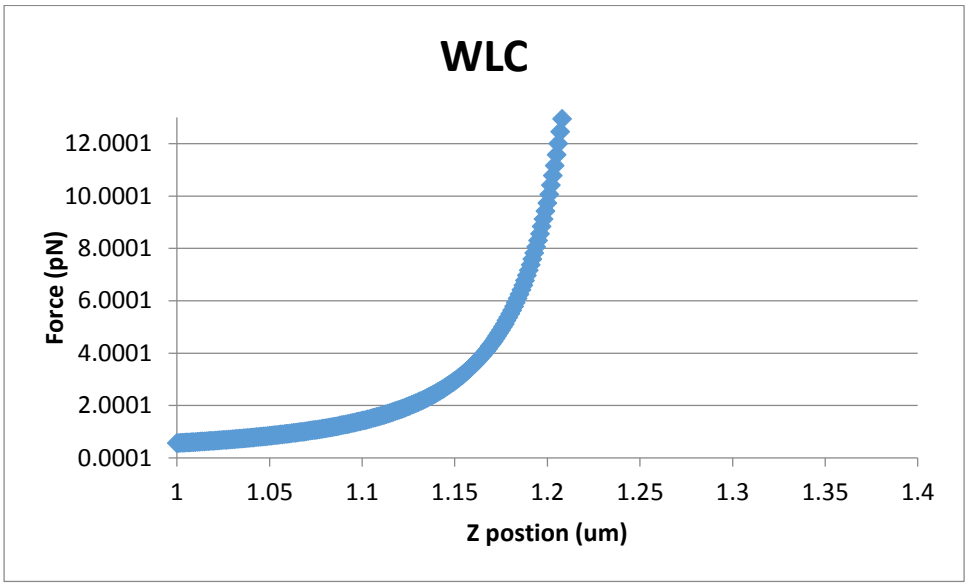

Figure 13: WLC with contracted Z range. The same values for the persistence length and contour length as in Figure 12 are used. For these parameters, we see much greater growth in the force than we do from the experimentally obtained data. It is difficult to say how the WLC would fit to the data obtained, as we do not see the full range of force possible with our version of the tweezers.

The first issue is most likely a result of not knowing with any precision where exactly the DNA is tethered to the bead. Figures 1 and 2 both assume an ideal attachment of the DNA to the bead, where the DNA is perfectly tethered to the bottom of the bead. Thus, when there is no magnetic force applied, the rest length extension of the DNA would be zero. In the non-ideal case, the DNA is attached or wrapped somewhere else than the bottom of the bead. In this case, the rest-length extension would be non-zero, because a portion of the DNA is physically extended by the fact that it is attached to the DNA. This could explain why we see a systematic offset of the DNA by about 1.1um before it begins to extend.

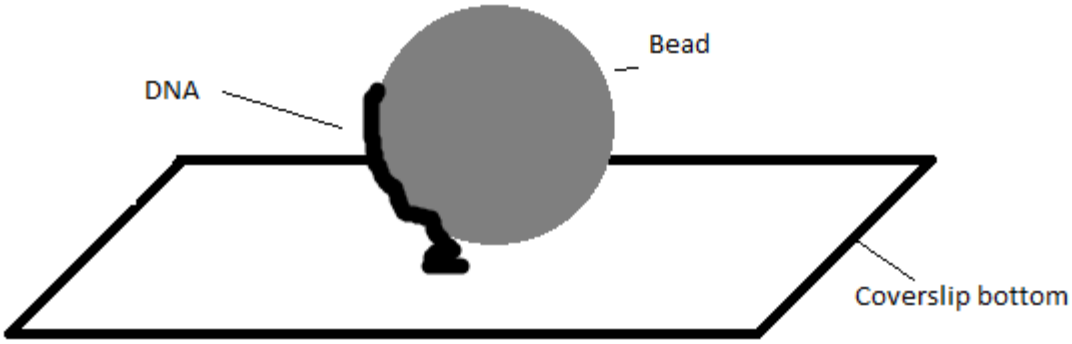

Figure 14: Cartoon Representation of Non-Ideal Tethering.

The results of the forward trace also show significant hysteresis of the bead during the pulling experiment. It's possible that these fluctuations of the bead are due to vibrations affecting the flow cell. While the MT setup currently sits on a floating table, the floating table was not floated during this experiment, and is not set up yet to run.

Dynamic force pulling experiments with the tweezers in the current state presents a little bit of difficulty. Currently, with the flow cell too thick to allow the magnets to come into physical contact with the flow cell, the calculation of the magnetic force does not represent the true maximum force that the magnets can apply to the beads. This means that a true force pulling curve cannot be constructed with some certainty. However, these results do show feasibility in the current version of the tweezers, and it is possible to obtain useful data following several improvements to the tweezers, such as the mentioned redesign of the flow cell, use of the floater table, and also the a mentioned use of piezo devices to control the position of the objective as opposed to the current stepper motor.

VI. Conclusion

The tweezers were used to conduct a simple dynamic force pulling experiment of DNA. The maximum force the tweezers were capable of exerting on the DNA was found to be 1.09 pN. The force extension curve was seen to match what would be suggested by increased magnetic force acting on a paramagnetic bead. However, there was a noted offset, which suggests that the DNA was not perfectly tethered to the bead.

There are also several improvements that can be made to the tweezers besides decreasing the thickness of the flow cell. The tweezers are mounted onto a floating table, which currently does not float. The addition of a working floater table can help to minimize any vibrations that will cause an adverse effect in the motion of the bead not do to Brownian motion or from the force of the magnets.

The removal of the stepper motors for the motion of the objective and its replacement with a piezo would also increase the accuracy of the objective's position. When moving the objective, there exist some slight fluctuations when arriving to a position, due to the motor under-damping the motor's acceleration. Thus, when it reaches its destination, it will oscillate about that destination for some time. Additionally, there exist bugs in the current version of the LabVIEW code that need to be properly identified and rectified. After these adjustments are made, it should be possible to do a dynamic force pulling experiment of DNA and actually fit the WLC to the force-extension curve. From this, it should be possible to determine the work done by the magnets on the DNA. Other potential future experiments include the extension of DNA under different salt conditions in the flow cell.

1. Neuman, Keir C., and Attila Nagy. “Single-Molecule Force Spectroscopy: Optical Tweezers, Magnetic Tweezers and Atomic Force Microscopy.” *Nature Methods* 5.6 (2008): 491–505. *PubMed Central*. Web. 31 Mar. 2015.

3. Abels, J. A. et al. “Single-Molecule Measurements of the Persistence Length of Double-Stranded RNA.” *Biophysical Journal* 88.4 (2005): 2737–2744. *ScienceDirect*. Web. 29 Apr. 2015.

4. Tempestini, A. et al. “Magnetic Tweezers Measurements of the Nanomechanical Stability of DNA against Denaturation at Various Conditions of pH and Ionic Strength.” *Nucleic Acids Research* 41.3 (2013): 2009–2019. *CrossRef*. Web. 29 Apr. 2015.

5. Zlatanova, Jordanka, and Sanford H. Leuba. “Magnetic Tweezers: A Sensitive Tool to Study DNA and Chromatin at the Single-Molecule Level.” *Biochemistry & Cell Biology* 81.3 (2003): 151. Print.

6. Lipfert, J. et al. “Magnetic torque tweezers: measuring torsional stiffness in DNA and RecA-DNA filmaments”. Advance Online Publication. *Nature Methods*. (2010). 29 Apr. 2015.

7. De Vlaminck, Iwijn et al. “Magnetic Forces and DNA Mechanics in Multiplexed Magnetic Tweezers.” *PLoS ONE* 7.8 (2012): e41432. *PLoS Journals*. Web. 22 Apr. 2015.

8. van Loenhout, M.T.J. “Single-molecule studies of the twisted, knotted, and broken genome”. Thesis. Delft University of Technology. (2012) Web. 29 Apr. 2015.

9. Gosse, Charlie, and Vincent Croquette. “Magnetic Tweezers: Micromanipulation and Force Measurement at the Molecular Level.” *Biophysical Journal* 82.6 (2002): 3314–3329. *ScienceDirect*. Web. 31 Mar. 2015.

10. Kruithof, M. et al. “Subpiconewton Dynamic Force Spectroscopy Using Magnetic Tweezers.” *Biophysical Journal* 94.6 (2008): 2343–2348. *ScienceDirect*. Web. 16 Apr. 2015.

11. Bouchiat, C. et al. “Estimating the Persistence Length of a Worm-Like Chain Molecule from Force-Extension Measurements.” *Biophysical Journal* 76.1 (1999): 409–413. *ScienceDirect*. Web. 29 Apr. 2015.

12. Segall, Darren E., Philip C. Nelson, and Rob Phillips. “Excluded-Volume Effects in Tethered-Particle Experiments: Bead Size Matters.” *Physical Review Letters* 96.8 (2006): 088306. Print.